Disentangling γ-ray observations of the Galactic Center using differentiable probabilistic programming

Siddharth Mishra-Sharma [* 1 2 3]   Tracy Robyn Slatyer [* 1 3]   Yitian Sun [* 1 3]   Yuqing Wu [* 4]

Abstract

We motivate the use of differentiable probabilistic programming techniques in order to account for the large model-space inherent to astrophysical γ-ray analyses. Targeting the longstanding Galactic Center γ-ray Excess (GCE) puzzle, we construct a differentiable forward model and likelihood that makes liberal use of GPU acceleration and vectorization in order to simultaneously account for a continuum of possible spatial morphologies consistent with the Excess emission in a fully probabilistic manner. Our setup allows for efficient inference over the large model space using variational methods. Beyond application to γ-ray data, a goal of this work is to showcase how differentiable probabilistic programming can be used as a tool to enable flexible analyses of astrophysical datasets.

1. Introduction

Analysis of γ-ray data towards the Galactic Center involves a subtle interplay between observations and theoretical models. The complexity of cosmic-ray transport processes in the region, combined with the fact that we only have access to a two-dimensional projection of this inherently three-dimensional process, means that we typically cannot make precise predictions about emission from many emitting sources. Consequently, scientific conclusions drawn from γ-ray analyses can depend strongly on specific assumptions made about the modeling of the signal and background, as well as manual choices involved in the data analysis pipeline.

---

[*]Equal contribution [1]Center for Theoretical Physics, Massachusetts Institute of Technology, Cambridge, USA [2]Department of Physics, Harvard University, Cambridge, USA [3]The NSF AI Institute for Artificial Intelligence and Fundamental Interactions (IAIFI), USA [4]Department of Physics, Imperial College London, UK. Correspondence to: Siddharth Mishra-Sharma <smsharma@mit.edu>, Yitian Sun <yitians@mit.edu>.

The γ-ray Galactic Center Excess (GCE), first identified over a decade ago (Goodenough & Hooper, 2009) using public data from the *Fermi*-LAT telescope (Atwood et al., 2009), is an excess of photons in the Inner Galaxy whose physical origin is currently unknown. Although the GCE has properties broadly compatible with those expected from annihilating dark matter (DM) (Goodenough & Hooper, 2009; Hooper & Goodenough, 2011; Daylan et al., 2016; Calore et al., 2015; Ajello et al., 2016), competing explanations in terms of a population of unresolved astrophysical point sources (PSs), in particular millisecond pulsars (MSPs), remain viable (Abazajian et al., 2014; Abazajian, 2011). Significant effort has gone into characterizing the GCE and understanding its origin, including through inferring the properties of unresolved PSs in the Inner Galaxy region. A particularly successful method in this direction, Non-Poissonian Template Fitting (NPTF), aims to characterize different populations of unresolved PSs using their photon statistics, via a likelihood-based analysis (Lee et al., 2015; 2016). In the context of the GCE, initial applications of this method showed overwhelming support for the hypothesis of the GCE being sourced by an unresolved population of PSs spatially correlated with the observed GCE morphology (Lee et al., 2016). However, more recent studies showed the method to be susceptible to systematic biases (Leane & Slatyer, 2019; 2020a;b; Chang et al., 2020) partly stemming from degeneracies between different emission components in the region (e.g., those spatially correlated with the GCE, centrally-concentrated stellar populations, and the Galactic disk), with results depending strongly on specific assumptions made about the spatial morphologies of components. *All NPTF analyses so far have assumed inflexible, spatially rigid templates, preventing a rigorous expression and exploration of this degeneracy.*

In this work, we use differentiable probabilistic programming as a means to alleviate this shortcoming of traditional likelihood-based fitting techniques for analyzing γ-ray data. Using GPU-native acceleration and vectorization, we construct a probabilistic forward model for γ-ray emission in the Galactic Center region that can generate high-resolution spatial templates for various emission components, including those associated with the GCE signal, on the fly during inference. This framework enables analyses that can be

more resilient to specific modeling choices by including a range of physically-reasonable variations on different emission components directly at the level of the forward model. In the broader context of astrophysical data analysis, this work aims to motivate the use of differentiable probabilistic programming as a way to enable high-dimensional Bayesian inference for complex descriptions of diverse astrophysical data.

2. Methodology

We describe our forward model and likelihood, its implementation as a differentiable probabilistic program, as well as the inference strategies used to perform Bayesian posterior inference.

2.1. The likelihood and forward model

In traditional spatial template fitting, photon counts x^p in different pixels p are modeled as Poisson random variables, with mean given by a linear combination of templates T_i^p, indexed i; $x^p \sim \text{Pois}\left(x^p \mid \sum_i A_i T_i^p\right)$. A_i are the template normalizations and represent the parameters of interest. The full map-level likelihood factorizes into a product of pixel-wise likelihoods, $p(x \mid \{A_i\}) = \prod_p p(x_p \mid \{A_i\})$.

In the presence of populations of unresolved PSs, the likelihood can be augmented to take into account the probability that a given pixel contains a PS from a given population, and the probability of that PS emitting a certain number of contributing photons. Point source populations can be independently characterized by a spatial distribution, specified by a template T_{PS}^p, and a source-count distribution $\mathrm{d}N/\mathrm{d}S$, which factorizes to describe the distribution of photon counts S from individual PSs, $p(S|\theta_{\text{PS}})$, and their mean abundance, $\bar{n}_{\text{PS}}$, as $\mathrm{d}N/\mathrm{d}S = \bar{n}_{\text{PS}}\, p(S \mid \theta_{\text{PS}})$.

Unfortunately, the inclusion of PS populations renders the likelihood intractable, since computing it would involve marginalizing over positions, photon counts, and the number of PSs from each population. The Non-Poissonian Template Fitting (NPTF) method (Lee et al., 2015; 2016) circumvents this issue by computing the pixel-wise likelihood accounting for the probability of finding a given number of sources in that pixel, but without seeking to include the positions of individual sources as latent variables; the full likelihood is approximated in a factorized form, $p\left(x \mid \bar{n}_{\text{PS}}, \theta_{\text{PS}}\right) = \prod_p p\left(x^p \mid \bar{n}_{\text{PS}}, \theta_{\text{PS}}\right)$. See Mishra-Sharma et al. (2017) for further details on the method. We implement a differentiable version of the NPTF likelihood using Jax (Bradbury et al., 2018), making liberal use of vectorization and automatic batching to efficiently compute the likelihood for multiple PS populations.

2.2. Flexible specification of point source populations

Previous analyses based on the NPTF framework assumed rigidly specified spatial templates for the distribution of PS populations; this is because generating new morphologies adds considerable overhead in the likelihood calculation, rendering a traditional Monte Carlo sampling-based analysis difficult. In particular, given a morphology for the PS template, $\rho(R, z)$ (assumed cylindrically symmetric), computing the template expectation in a given pixel p involves performing a line-of-sight integral in the pixel direction. In Jax, the density over the line of sight as well across the pixel index can be efficiently vectorized, and the computation is just-in-time (JIT) compiled for efficient execution on a GPU.

This allows us to include parametric variations on different spatial templates that have been previously included in NPTF analyses, including templates for PSs correlated with the Galactic disk and the GCE, directly as part of the inference pipeline. We model a PS population with a generalized Navarro-Frenk-White (NFW) profile, motivated by the DM expectation: $\rho_{\text{NFW}}(r) \propto (r/r_s)^{-\gamma} (1 + r/r_s)^{-3+\gamma}$ with the inner slope γ a free parameter to be inferred during the analysis, and r_s a fixed scale radius.

We also model a population of PSs spatially correlated with the Galactic disk, modeled using a cylindrically symmetric, doubly exponential profile (Bartels et al., 2018; Lorimer et al., 2006), $\rho_{\text{disk}}(R, z) \propto R^B \exp\left[-C\left(R - R_\odot\right)/R_\odot\right] \exp\left(-|z|/z_s\right)$ with the parameter B, C, and the scale height z_s characterizing the disk morphology to be inferred during the analysis. $R_\odot$ is the distance of the Sun from the Galactic Center.

The possibility of a population of PSs correlated with the stellar density in the Galactic bulge has been extensively tested in the literature (Macias et al., 2018; 2019; Ploeg et al., 2020), with different analyses finding divergent results for whether this scenario is preferred. We allow for this possibility in our analysis by including multiple publicly-available spatial templates following stellar bulge populations (Macias et al., 2018; Coleman et al., 2020; Macias et al., 2019; McDermott et al., 2023) For both the PS as well as smooth (Poissonian) components describing the GCE, we model the spatial distribution as a hybrid template allowing for varying fractions of DM-like and bulge-like morphologies, $T_{\text{GCE}}^p = (1 - f_{\text{bulge}})T_{\text{DM}}^p + f_{\text{bulge}}T_{\text{bulge}}^p$. The bulge template itself is modeled as a linear combination of publicly available bulge morphologies, $T_{\text{bulge}}^p = \sum_i \alpha_i T_{\text{bulge},i}^p$ with α_i modeled with a symmetric Dirichlet prior, enforcing $\sum_i \alpha_i = 1$. The templates are appropriately normalized such that an un-scaled template would produce one count per pixel, allowing for a physically-meaningful interpretation of the bulge fraction f_{bulge} parameter as the relative contribution to the GCE PS or smooth component from the

composite bulge component. A graphical representation of the model of the spatial morphology of the GCE, as specified for both the PS as well as smooth components, is shown in Fig. 1.
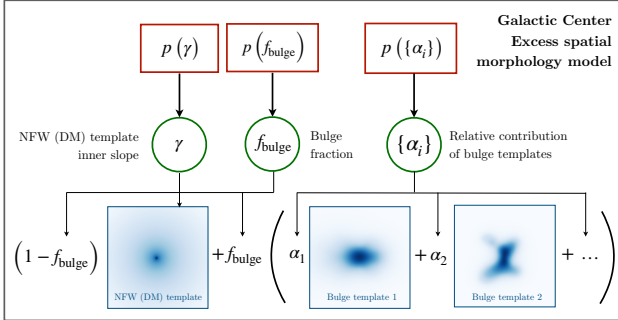
Figure 1. Graphical model of the spatial morphology of the Galactic Center Excess, as specified for both the PS as well as smooth emission components.

2.3. Parameter posterior inference

Since the entire pipeline from template generation to likelihood evaluation is end-to-end differentiable, we can evaluate gradients of the log-likelihood function with respect to the parameters of interest θ characterizing the smooth as well as PS components, $\nabla_\theta \log p(x \mid \theta)$, with minimal overhead. This opens up the possibility of using highly efficient gradient-based posterior inference techniques like Stochastic Variational Inference (SVI) (Hoffman et al., 2012) and Hamiltonian Monte Carlo (HMC) (Hoffman & Gelman, 2011). Unlike traditional sampling techniques previously employed in the context of *Fermi* GCE analyses, these methods can easily scale up to high-dimensional parameter spaces. In particular, variational methods turn posterior inference into an optimization problem by fitting for a flexible functional ansatz on the posterior density and can easily deal with hundreds of parameters. This is in contrast to current public implementations of NPTF, which cannot efficiently include real-time generated templates at inference and are restricted to a modest number of parameters with traditional Monte Carlo sampling techniques. The constructed likelihood is wrapped using the probabilistic programming framework `NumPyro` (Phan et al., 2019), which allows for flexible specification of complex forward models as well as performing inference on them using gradient-based techniques.

In stochastic variational inference (SVI) an approximation for the posterior distribution, parameterized by φ and denoted $q_\varphi(\theta)$, is obtained by minimizing the reverse KL-divergence between the true and variational posterior distributions, $D_{\mathrm{KL}}(q_\varphi \mid\mid p(\theta \mid x))$. This is done by maximizing the model log-evidence $\log p(x)$ or, in practice using

the tractable evidence lower bound (ELBO), $\mathrm{ELBO} \equiv \mathbb{E}_{\vartheta \sim q_\varphi(\theta)}[\log p(x, \theta) - \log q_\varphi(\theta)]$, as the optimization objective since $\log p(x) - \mathrm{ELBO} = D_{\mathrm{KL}}(q_\varphi \mid\mid p(\theta \mid x))$. The expectation in the ELBO is taken through Monte Carlo sampling from the variational distribution at each optimization step.

Since we seek the capability to model arbitrarily flexible non-Gaussian posterior distributions, the variational family q_φ is modeled using an inverse autoregressive normalizing flow (IAF) (Kingma et al., 2016) consisting of 5 flow transformations modeled using masked autoencoders consisting of two 128-dimensional hidden layers with tanh nonlinearities. The variational parameters – the parameters of the normalizing flow transformation – are optimized using `Optax` (Hessel et al., 2020) with the AdamW optimizer (Kingma & Ba, 2014; Loshchilov & Hutter, 2017) over 7,500 steps initial learning rate 10^{-4}. Optimization typically takes ~ 10 minutes on a single Nvidia A100 GPU.

3. Experiments and results

We apply our pipeline to 573 weeks of *Fermi*-LAT data in the 2–20 GeV energy range. Smooth templates corresponding to isotropically-uniform emission, emission from (resolved) PSs in the 3FGL catalog (Acero et al., 2015), and the *Fermi* bubbles (Su et al., 2010) are included. Three different diffuse models – Models 'A' and 'F' from Calore et al. (2015) and Model 'O' from Macias et al. (2019) – are used to model the Galactic diffuse foreground emission, with the gas-correlated emission and Galactic charge density-correlated emission separately modeled as linear combinations of the corresponding components of the three templates. Following (Buschmann et al., 2020), we allow for a modulation of the large-scale spatial structure of the gas-correlated templates modifying it as $T_{\mathrm{diff}}^p \rightarrow [1 + \sum_{\ell m} A_{\ell m} \cdot \mathrm{Re}(Y_{\ell m}^p)] T_{\mathrm{diff}}^p$, where the prior on spherical harmonic coefficients $A_{\ell m}$ enforces small deviations from the base template; $p(A_{\ell m}) = \mathcal{U}(-0.05, 0.05)$.

In total, our fiducial model is characterized by 42 parameters of interest: 15 normalization parameters for the smooth emission templates; 6 spherical harmonic coefficients (up to $l = 2$); 1 inner slope parameter for the smooth NFW template; 7 normalization parameters for PS templates (5 for bulge templates, 1 each for the disk and the NFW); 10 parameters for the source-count distributions for the GCE and the disk PS populations (3 slopes, 2 spectral breaks each); 2 shape parameters for the disk PS template; and 1 inner slope parameter for the PS NFW component.

The region of interest is taken to be the inner $25°$, masking the Galactic plane at $2°$. Resolved PSs from the 3FGL catalog are masked at $0.8°$. `HEALPix` (Gorski et al., 2005) pixelization with resolution parameter `nside = 128` is
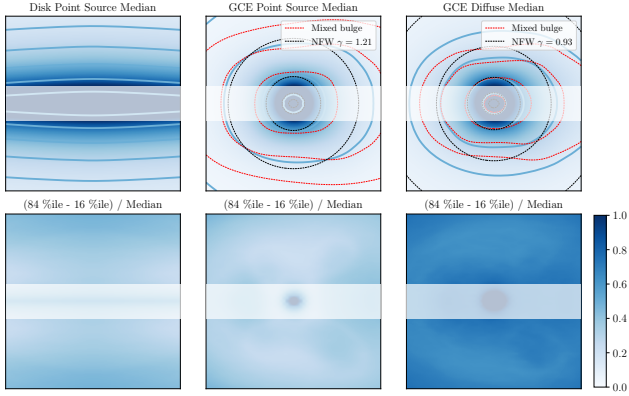
Figure 2. Summaries of the inferred posteriors for disk-correlated PS, GCE-correlated PS, and GCE-correlated smooth emission morphologies from a preliminary analysis of *Fermi*-LAT data. The top row shows the median inferred pixel-wise morphologies, while the bottom row shows the relative middle-68% deviation of the posterior from the median. For comparison, contours for the best-fitting bulge and DM (NFW) description are shown for the GCE PS and smooth components.

used, corresponding to pixels of side $\sim 0.5°$ and a total of 6839 pixels in the region of interest.

Figures 2 and 3 summarize preliminary results obtained using our pipeline applied to Inner Galaxy *Fermi* data. Summaries of the inferred posteriors for disk-correlated PS, GCE-correlated PS, and GCE-correlated smooth emission morphologies are shown in Fig. 2. The top row shows the median inferred pixel-wise morphologies, while the bottom row shows the relative middle-68% deviation of the posterior from the median (heuristically, the '1-σ' range of the posterior distribution). Contours for the best-fitting bulge-correlated (dotted red lines) and DM-like (dotted black lines) components are shown. It can be seen that, for both PS-like as well as smooth emission, the inferred posterior median is fairly spherically symmetric when contrasted to the bulge profile expectation; this reflects a general preference for DM-like morphologies in our analyses. We emphasize that we obtain a full posterior distribution over preferred signal morphologies, departing significantly from the rigid parametric descriptions used in previous works.

Figure 3 shows posteriors on select parameters characterizing the GCE and disk PS morphologies. The bulge fraction $f_{\rm bulge,PS} \sim 0.3$ quantitatively substantiates a modest preference for a DM-like morphology in the GCE emission. Posteriors on the NFW inner slopes γ for the PS and smooth NFW profiles, as well as select parameters characterizing the disk morphology are shown. A physically-reasonable scale height for the disk-correlated PS population, $z_s \sim 0.4\,$kpc is inferred (Bartels et al., 2018). Overall,

our preliminary analysis assigns $73^{+9}_{-6}\%$ of the total GCE flux to unresolved PS-like structure.

4. Discussion and outlook

We have introduced a scalable and flexible pipeline for disentangling the contribution of various emission components to the observed γ-ray sky using differentiable probabilistic programming. The pipeline makes extensive use of the seamless vectorization, automatic differentiation, just-in-time compilation, and GPU acceleration enabled by the Jax framework as well as the flexible model specification and inference capabilities of the NumPyro. In a preliminary analysis, we applied our pipeline to Inner Galaxy *Fermi*-LAT γ-ray data with the goal of characterizing the longstanding GCE emission while allowing for a richer description of possible signal morphologies and Galactic foreground model descriptions.
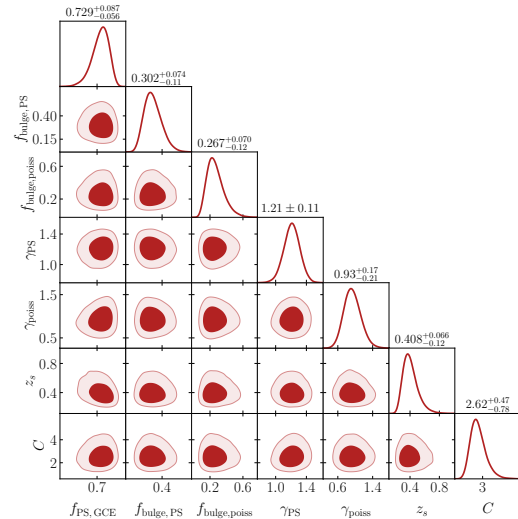
Figure 3. Posteriors on select parameters characterizing the GCE and disk PS morphologies obtained with a preliminary analysis of *Fermi*-LAT data in the Inner Galaxy. The PS fraction of the GCE $f_{\rm PS,\,GCE}$, the bulge fractions $f_{\rm bulge}$ within the PS GCE components and the smooth GCE components, NFW inner slopes γ for the PS and smooth NFW profiles, as well as parameters characterizing the disk PSs morphology are shown.

We outline possible extensions to the pipeline. While we have used parametric and physically-motivated morphologies for the spatial distribution of various PS populations, using our pipeline we will be able to characterize Galactic Center in a fully signal model-independent manner by scanning over a space of spatial functions on the sky map e.g., using Gaussian processes (GPs) to define the function prior. A similar GP-based technique was implemented in Mishra-Sharma & Cranmer (2020) to augment the morphology of the diffuse foreground template. Finally, since our pipeline is implemented using differential programming, it can admit

arbitrarily flexible descriptions of the Galactic foreground emission, e.g. as a latent-variable generative model that spans a distribution of possible foreground models. We leave a study of these extensions to future work.

Acknowledgements

References

Abazajian, K. N. The Consistency of Fermi-LAT Observations of the Galactic Center with a Millisecond Pulsar Population in the Central Stellar Cluster. *JCAP*, 03:010, 2011. doi: 10.1088/1475-7516/2011/03/010.

Abazajian, K. N., Canac, N., Horiuchi, S., and Kaplinghat, M. Astrophysical and Dark Matter Interpretations of Extended Gamma-Ray Emission from the Galactic Center. *Phys. Rev. D*, 90(2):023526, 2014. doi: 10.1103/PhysRevD.90.023526.

Acero, F. et al. Fermi Large Area Telescope Third Source Catalog. *Astrophys. J. Suppl.*, 218(2):23, 2015. doi: 10.1088/0067-0049/218/2/23.

Ajello, M. et al. Fermi-LAT Observations of High-Energy γ-Ray Emission Toward the Galactic Center. *Astrophys. J.*, 819(1):44, 2016. doi: 10.3847/0004-637X/819/1/44.

Atwood, W. B. et al. The Large Area Telescope on the Fermi Gamma-ray Space Telescope Mission. *Astrophys. J.*, 697: 1071–1102, 2009. doi: 10.1088/0004-637X/697/2/1071.

Bartels, R., Edwards, T., and Weniger, C. Bayesian model comparison and analysis of the galactic disc population of gamma-ray millisecond pulsars. *Monthly Notices of the Royal Astronomical Society*, 481(3):3966–3987, 2018.

Bradbury, J., Frostig, R., Hawkins, P., Johnson, M. J., Leary, C., Maclaurin, D., Necula, G., Paszke, A., VanderPlas, J., Wanderman-Milne, S., and Zhang, Q. JAX: composable transformations of Python+NumPy programs, 2018. URL http://github.com/google/jax.

Buschmann, M., Rodd, N. L., Safdi, B. R., Chang, L. J., Mishra-Sharma, S., Lisanti, M., and Macias, O. Foreground Mismodeling and the Point Source Explanation of the Fermi Galactic Center Excess. *Phys. Rev. D*, 102 (2):023023, 2020. doi: 10.1103/PhysRevD.102.023023.

Calore, F., Cholis, I., and Weniger, C. Background Model Systematics for the Fermi GeV Excess. *JCAP*, 03:038, 2015. doi: 10.1088/1475-7516/2015/03/038.

Chang, L. J., Mishra-Sharma, S., Lisanti, M., Buschmann, M., Rodd, N. L., and Safdi, B. R. Characterizing the nature of the unresolved point sources in the Galactic Center: An assessment of systematic uncertainties. *Phys. Rev. D*, 101(2):023014, 2020. doi: 10.1103/PhysRevD. 101.023014.

Coleman, B., Paterson, D., Gordon, C., Macias, O., and Ploeg, H. Maximum entropy estimation of the galactic bulge morphology via the vvv red clump. *Monthly Notices of the Royal Astronomical Society*, 495(3):3350–3372, 2020.

Daylan, T., Finkbeiner, D. P., Hooper, D., Linden, T., Portillo, S. K. N., Rodd, N. L., and Slatyer, T. R. The characterization of the gamma-ray signal from the central Milky Way: A case for annihilating dark matter. *Phys. Dark Univ.*, 12:1–23, 2016. doi: 10.1016/j.dark.2015.12.005.

Goodenough, L. and Hooper, D. Possible Evidence For Dark Matter Annihilation In The Inner Milky Way From The Fermi Gamma Ray Space Telescope. 10 2009.

Gorski, K. M., Hivon, E., Banday, A. J., Wandelt, B. D., Hansen, F. K., Reinecke, M., and Bartelman, M. HEALPix - A Framework for high resolution discretization, and fast analysis of data distributed on the sphere. *Astrophys. J.*, 622:759–771, 2005. doi: 10.1086/427976.

Hessel, M., Budden, D., Viola, F., Rosca, M., Sezener, E., and Hennigan, T. Optax: composable gradient transformation and optimisation, in jax!, 2020. URL http://github.com/deepmind/optax.

Hoffman, M., Blei, D. M., Wang, C., and Paisley, J. Stochastic Variational Inference. *arXiv e-prints*, art. arXiv:1206.7051, June 2012. doi: 10.48550/arXiv.1206. 7051.

Hoffman, M. D. and Gelman, A. The No-U-Turn Sampler: Adaptively Setting Path Lengths in Hamiltonian Monte Carlo. *arXiv e-prints*, art. arXiv:1111.4246, November 2011. doi: 10.48550/arXiv.1111.4246.

Hooper, D. and Goodenough, L. Dark Matter Annihilation in The Galactic Center As Seen by the Fermi Gamma Ray Space Telescope. *Phys. Lett. B*, 697:412–428, 2011. doi: 10.1016/j.physletb.2011.02.029.

Kingma, D. P. and Ba, J. Adam: A method for stochastic optimization. *arXiv preprint arXiv:1412.6980*, 2014.

Kingma, D. P., Salimans, T., Jozefowicz, R., Chen, X., Sutskever, I., and Welling, M. Improved variational inference with inverse autoregressive flow. In *Proceedings of the 30th International Conference on Neural Information Processing Systems*, NIPS'16, pp. 4743–4751, Red Hook, NY, USA, 2016. Curran Associates Inc. ISBN 9781510838819. URL https://papers.nips.cc/paper/2016/hash/ddeebdeefdb7e7e7a697e1c3e3d8ef54-Abstract.html.

Leane, R. K. and Slatyer, T. R. Revival of the Dark Matter Hypothesis for the Galactic Center Gamma-Ray Excess. *Phys. Rev. Lett.*, 123(24):241101, 2019. doi: 10.1103/PhysRevLett.123.241101.

Leane, R. K. and Slatyer, T. R. Spurious Point Source Signals in the Galactic Center Excess. *Phys. Rev. Lett.*, 125(12):121105, 2020a. doi: 10.1103/PhysRevLett.125.121105.

Leane, R. K. and Slatyer, T. R. The enigmatic Galactic Center excess: Spurious point sources and signal mismodeling. *Phys. Rev. D*, 102(6):063019, 2020b. doi: 10.1103/PhysRevD.102.063019.

Lee, S. K., Lisanti, M., and Safdi, B. R. Distinguishing Dark Matter from Unresolved Point Sources in the Inner Galaxy with Photon Statistics. *JCAP*, 05:056, 2015. doi: 10.1088/1475-7516/2015/05/056.

Lee, S. K., Lisanti, M., Safdi, B. R., Slatyer, T. R., and Xue, W. Evidence for Unresolved γ-Ray Point Sources in the Inner Galaxy. *Phys. Rev. Lett.*, 116(5):051103, 2016. doi: 10.1103/PhysRevLett.116.051103.

Lorimer, D. R., Faulkner, A., Lyne, A., Manchester, R. N., Kramer, M., McLaughlin, M., Hobbs, G., Possenti, A., Stairs, I., Camilo, F., et al. The parkes multibeam pulsar survey–vi. discovery and timing of 142 pulsars and a galactic population analysis. *Monthly Notices of the Royal Astronomical Society*, 372(2):777–800, 2006.

Loshchilov, I. and Hutter, F. Decoupled weight decay regularization. *arXiv preprint arXiv:1711.05101*, 2017.

Macias, O., Gordon, C., Crocker, R. M., Coleman, B., Paterson, D., Horiuchi, S., and Pohl, M. Galactic bulge preferred over dark matter for the Galactic centre gamma-ray excess. *Nature Astron.*, 2(5):387–392, 2018. doi: 10.1038/s41550-018-0414-3.

Macias, O., Horiuchi, S., Kaplinghat, M., Gordon, C., Crocker, R. M., and Nataf, D. M. Strong Evidence that the Galactic Bulge is Shining in Gamma Rays. *JCAP*, 09: 042, 2019. doi: 10.1088/1475-7516/2019/09/042.

McDermott, S. D., Zhong, Y.-M., and Cholis, I. On the morphology of the gamma-ray galactic centre excess. *Monthly Notices of the Royal Astronomical Society: Letters*, 522(1):L21–L25, 2023.

Mishra-Sharma, S. and Cranmer, K. Semi-parametric γ-ray modeling with Gaussian processes and variational inference. 10 2020.

Mishra-Sharma, S., Rodd, N. L., and Safdi, B. R. NPTFit: A code package for Non-Poissonian Template Fitting. *Astron. J.*, 153(6):253, 2017. doi: 10.3847/1538-3881/aa6d5f.

Phan, D., Pradhan, N., and Jankowiak, M. Composable Effects for Flexible and Accelerated Probabilistic Programming in NumPyro. *arXiv e-prints*, art. arXiv:1912.11554, December 2019. doi: 10.48550/arXiv.1912.11554.

Ploeg, H., Gordon, C., Crocker, R., and Macias, O. Comparing the Galactic Bulge and Galactic Disk Millisecond Pulsars. *JCAP*, 12:035, 2020. doi: 10.1088/1475-7516/2020/12/035.

Su, M., Slatyer, T. R., and Finkbeiner, D. P. Giant Gamma-ray Bubbles from Fermi-LAT: AGN Activity or Bipolar Galactic Wind? *Astrophys. J.*, 724:1044–1082, 2010. doi: 10.1088/0004-637X/724/2/1044.